

## **CLITORIA TERNATEA - MEDIATED ZnO NANOPARTICLES FOR ENZYME-FREE PHOTOELECTROCHEMICAL CHOLESTEROL DETECTION**

*Sushmitha S<sup>a</sup>, Lavanya Rao<sup>a</sup>, Mahesha P Nayak<sup>a</sup>, Shreeganesch Subraya Hegde<sup>b</sup>, Badekai Ramachandra Bhat<sup>a\*</sup>*

*<sup>a</sup> Department of Chemistry, Catalysis and Materials Chemistry Laboratory, National Institute of Technology Karnataka, Surathkal, D.K., Karnataka 575 025, India.*

*<sup>b</sup> Department of Chemistry, School of Engineering, Dayananda Sagar University, Harohalli, Bengaluru, Karnataka 562112, India*

*\*Corresponding Author: [ram@nitk.edu.in](mailto:ram@nitk.edu.in)*

### **1. Experimental Details**

#### **1.1 Chemicals and Materials**

Nickel Foam ((NF), Thickness 0.5mm, 99.9% Purity) purchased from Global Nanotech, Mumbai. Zinc nitrate hexahydrate ( $\text{Zn}(\text{NO}_3)_2 \cdot 6\text{H}_2\text{O}$ , 99% crystalline), Sodium hydroxide flakes (NaOH, 97% Extra Pure), Potassium Hydroxide Pellets (KOH, 85% Extra Pure), Uric Acid ((UA),  $\text{C}_5\text{H}_4\text{N}_4\text{O}_3$ , 99% AR), Cholesterol ( $\text{C}_{27}\text{H}_{46}\text{O}$ , 97% Extra Pure), L-Ascorbic Acid ((AA),  $\text{C}_6\text{H}_8\text{O}_6$ , 99% Extra Pure), N-Methyl 2-Pyrrolidone ((NMP),  $\text{C}_5\text{H}_9\text{NO}$ , 98% Purity), and Dextrose Anhydrous (D-(+)-Glucose,  $\text{C}_6\text{H}_{12}\text{O}_6$ , extra pure) were purchased from LOBA Chemie Pvt. Ltd. Dopamine Hydrochloride (DA), Poly (Vinylidene Fluoride) (PVDF), Triton™ X – 100, and Creatinine anhydrous ( $\leq 98\%$ ) was procured through Sigma-Aldrich, Germany. Ultra-pure Milli-Q water (Elga Veolia) was utilised throughout the experiment. All chemicals were analytically certified and used without filtering.

#### **1.2 Extract Preparation**

Fresh flowers (10 g) were thoroughly cleaned and rinsed once with Milli-Q water to remove surface impurities. The cleaned flowers were then boiled in 100 mL of Milli-Q water at 80 °C for 30 minutes. During the extraction process, a noticeable colour changes from transparent to dark blue was observed. The obtained extract was filtered to remove any solid particles and stored for further use.

### 1.3 Electrode Fabrication

The synthesised product was blended with PVDF in a 9:1 weight ratio and thoroughly ground using a mortar and pestle to obtain a homogeneous mixture. NMP was added dropwise to the mixture to form a uniform paste. This paste was then evenly coated onto a pre-treated NF substrate within a defined area of  $1 \times 1 \text{ cm}^2$ . The fabricated electrode was subsequently dried in a vacuum oven at  $60 \text{ }^\circ\text{C}$  for 24 hours. The final mass coated on the NF surface was determined to be  $10 \pm 0.2 \text{ mg}$ .

### 1.4 Material and Electrochemical Characterisation

The structural property of the synthesised material was characterised using a Rigaku Miniflex 600 powder X-ray diffraction (XRD) device, and the crystallite size ( $D$ ) was calculated using the Debye-Scherrer equation. (Eq. 1)

$$D = \frac{K\lambda}{\beta \cos \theta} \quad (1)$$

Here,  $K$  is the Scherrer constant,  $\lambda$  is the Cu- $K\alpha$  radiation wavelength,  $\beta$  is the full width at half maximum (FWHM) of the peak, and  $\theta$  is the Bragg angle. Phonon vibration and optical absorption spectra were analysed using a Renishaw Raman Spectrometer and UV-vis-NIR, Lambda 950, Perkin Elmer. Additionally, morphological studies were examined using a 7610FPPLUS, Jeol, field emission scanning electron microscope (FESEM). Elemental analysis was carried out in Inductively Coupled Plasma Mass Spectrometry (ICP-MS) NexION 2000, Perkin Elmer, BET Autosorb IQ-XR-XR, Anton Paar.

All the Electrochemical studies were carried out using a three-electrode setup with fabricated NF acting as the working electrode (WE), a platinum electrode as the counter electrode (CE), and a saturated Ag/AgCl electrode as the reference electrode in 0.1 M KOH using an Autolab PGSTAT204 electrochemical workstation. CV studies were carried out within a potential window of 0.2 to 0.75 V (vs. Ag/AgCl) at scan rates ranging from 5 to 120 mV/s. CA analysis was conducted by successive additions of cholesterol under continuous stirring at a specified applied potential (vs. Ag/AgCl). DPV (Differential Pulse Voltammetry) was performed in the potential range of 0.35 to 0.65 V (vs. Ag/AgCl) with a scan rate of 10 mV/s and a pulse amplitude of 50 mV. LSV (Linear Sweep Voltammetry) was performed in the potential range of 0.5 to 0.8 V (vs. Ag/AgCl) with a scan rate of 50 mV/s. The ECSA was estimated by

recording CVs at scan rates between 5 and 75 mV/s within a selected potential window. The double-layer capacitance ( $C_{dl}$ ) was determined by plotting  $\Delta j$  (where  $\Delta j = j_a - j_c$ ) against the scan rate. The accurate surface area was then calculated using the formula  $C_{dl}/C_s$ <sup>1</sup>, where  $C_s$  is the capacitance of an atomically smooth surface, taken as 40  $\mu\text{F}\cdot\text{cm}^{-2}$ <sup>2,3</sup>. The light study was performed in illuminated mode by using a Philips Master Colour CDM-R PAR30L 70 W, Ceramic Metal Halide (CDM) Lamp light source. The sensitivity of the electrode towards cholesterol detection was determined from the slope of the calibration curve obtained by plotting the current response against varying cholesterol concentrations, as represented by **Eq. 2**.

$$\text{Sensitivity} = \frac{\text{Slope of the calibration curve}}{\text{Surface area}} \quad (2)$$

The formulas used to calculate LOD and LOQ are represented by (**Eq. 3 and 4**).

$$\text{LOD} = \frac{3 \times \text{Standard deviation}}{\text{Slope of the calibration curve}} \quad (3)$$

$$\text{LOQ} = \frac{10 \times \text{Standard deviation}}{\text{Slope of the calibration curve}} \quad (4)$$

**Table S1:** Comparative table analysing the electrochemical performance against previously reported sensors on green synthesis.

Material / System	Green Source	Target Analyte	Sensitivity	Detection Limit	Ref.
Ag and Au NPs	<i>Rumex roseus</i>	H <sub>2</sub> O <sub>2</sub> and riboflavin	64 mA mM <sup>-1</sup>	1.1 μM	4
phosphorus and nitrogen dual carbon Quantum dots	<i>banana flower bract extract</i>	dopamine	16.68 μA μM <sup>-1</sup> cm <sup>-2</sup>	500 pM	5
cadmium oxide nanoparticles	<i>Nymphaea Alba</i>	cefixime	-	0.06 μmol L <sup>-1</sup>	6
Manganese oxide	<i>Syzygium aromaticum</i>	<i>p</i> -nitrophenol	0.16 μA μM <sup>-1</sup> cm <sup>2</sup>	15.65 μM	7
reduced graphene oxide	<i>cow urine</i>	glucose	19.17 μA cm <sup>-2</sup> mM <sup>-1</sup>	1.9019 μM	8
lanthanum vanadate	<i>Colocasia esculenta</i>	paracetamol	187.25 μA μM <sup>-1</sup> cm <sup>-2</sup> and 3267.46 μA μM <sup>-1</sup> cm <sup>-2</sup>	0.0182 μM	9
NiO-Co <sub>3</sub> O <sub>4</sub> nanocomposites	<i>tea leaf extract</i>	glucose	1934.2 μA · mM <sup>-1</sup> · cm <sup>-2</sup>	0.15 μM	10
ZnO nanoparticles	<i>Clitoria ternatea</i>	Cholesterol	Dark: 492.5 μA mM <sup>-1</sup> cm <sup>-2</sup>	35 μM	<b>This work</b>
			Light: 956 μA mM <sup>-1</sup> cm <sup>-2</sup>	28 μM	

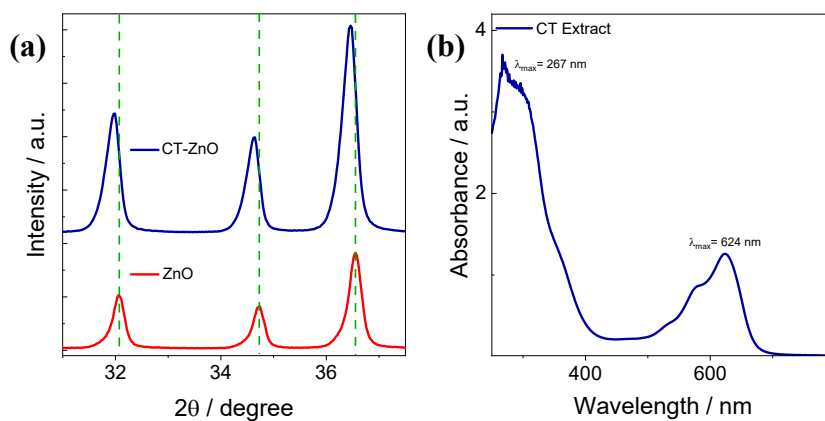


**Figure S1:** (a) shift of the (100), (002), and (101) XRD peaks to lower diffraction angles due to incorporation of CT-flower extract; (b) UV-Vis spectrum of diluted CT flower extract

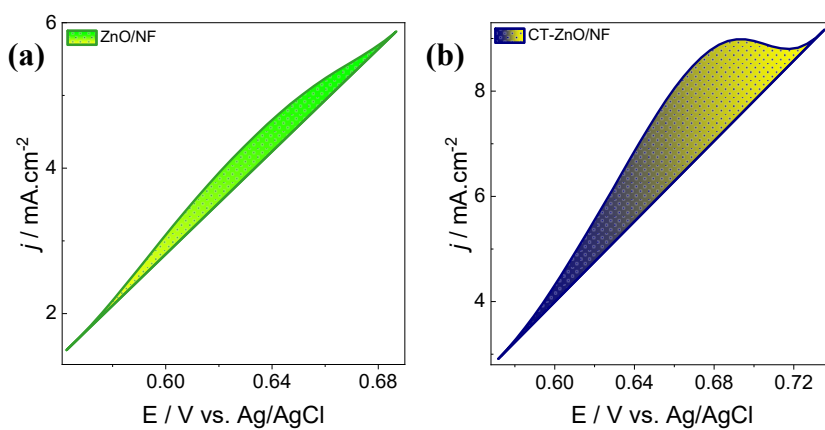


**Figure S2:** Oxidation peak study of (a) ZnO/NF; (b) CT-ZnO/NF.

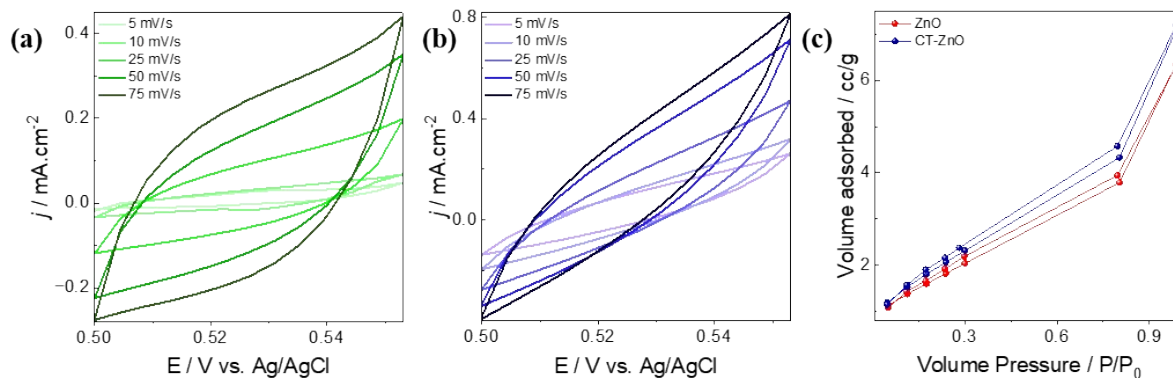


**Figure S3:** ECSA analysis of (a) ZnO/NF; (b) CT-ZnO/NF; (c) BET analysis of ZnO and CT-ZnO.

Material	Slope ( $\mu\text{F}\cdot\text{cm}^{-2}$ )	(Slope / $40 \times 2$ ) ( $\text{cm}^2$ )
<b>ZnO</b>	<b>4.35</b>	<b>0.054</b>
<b>CT-ZnO</b>	<b>4.6</b>	<b>0.058</b>

**Table S2:** Surface Area Calculation

**Table S3:** EIS parameters for the fitted Circuit

Parameters	ZnO/NF	CT-ZnO/NF
Rs	9.841	1.008
Qct	2.85	1.61
Rct	8.8	2.94
Qcdl	0.64	0.47
Rcdl	1859	283.9
Cir	9.66	1.47
Rir	1.93	1.55

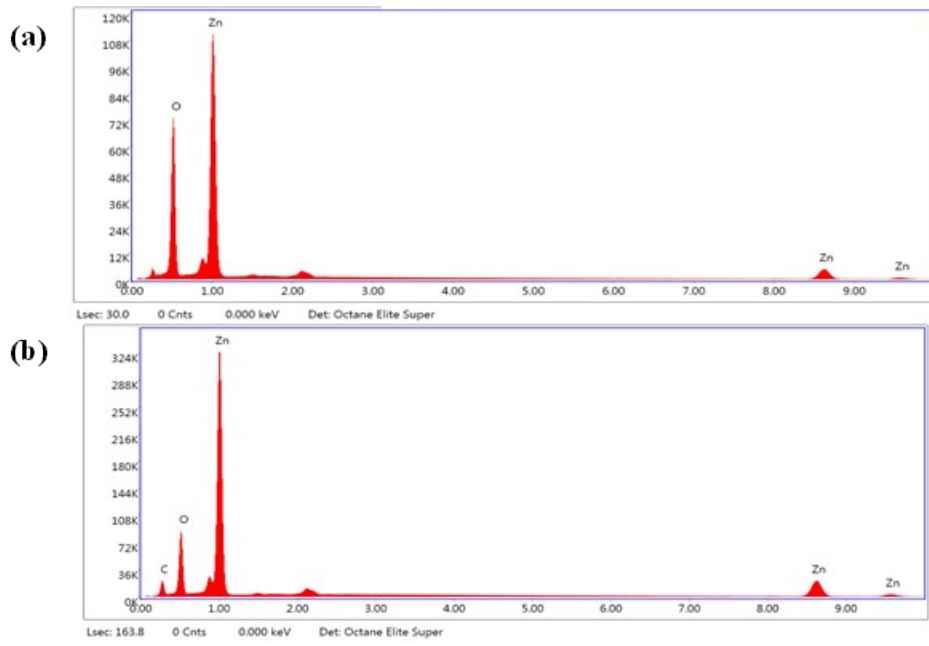


**Figure S4:** EDAX analysis of (a) ZnO; (b) CT-ZnO.

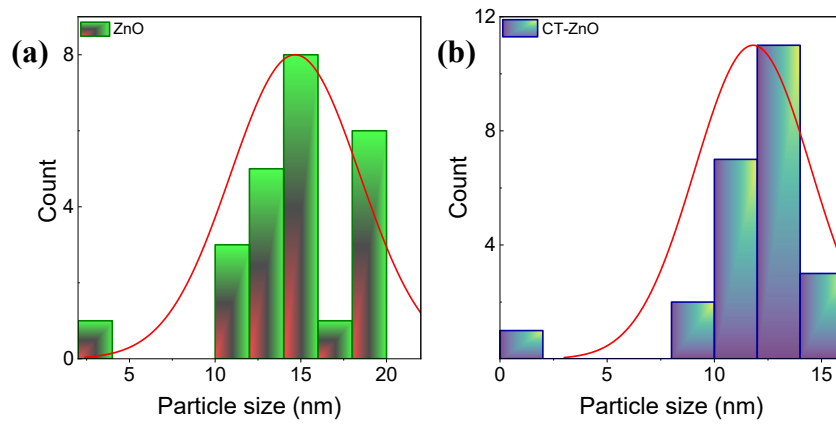


**Figure S5:** Particle size distribution of (a) ZnO; (b) CT-ZnO.

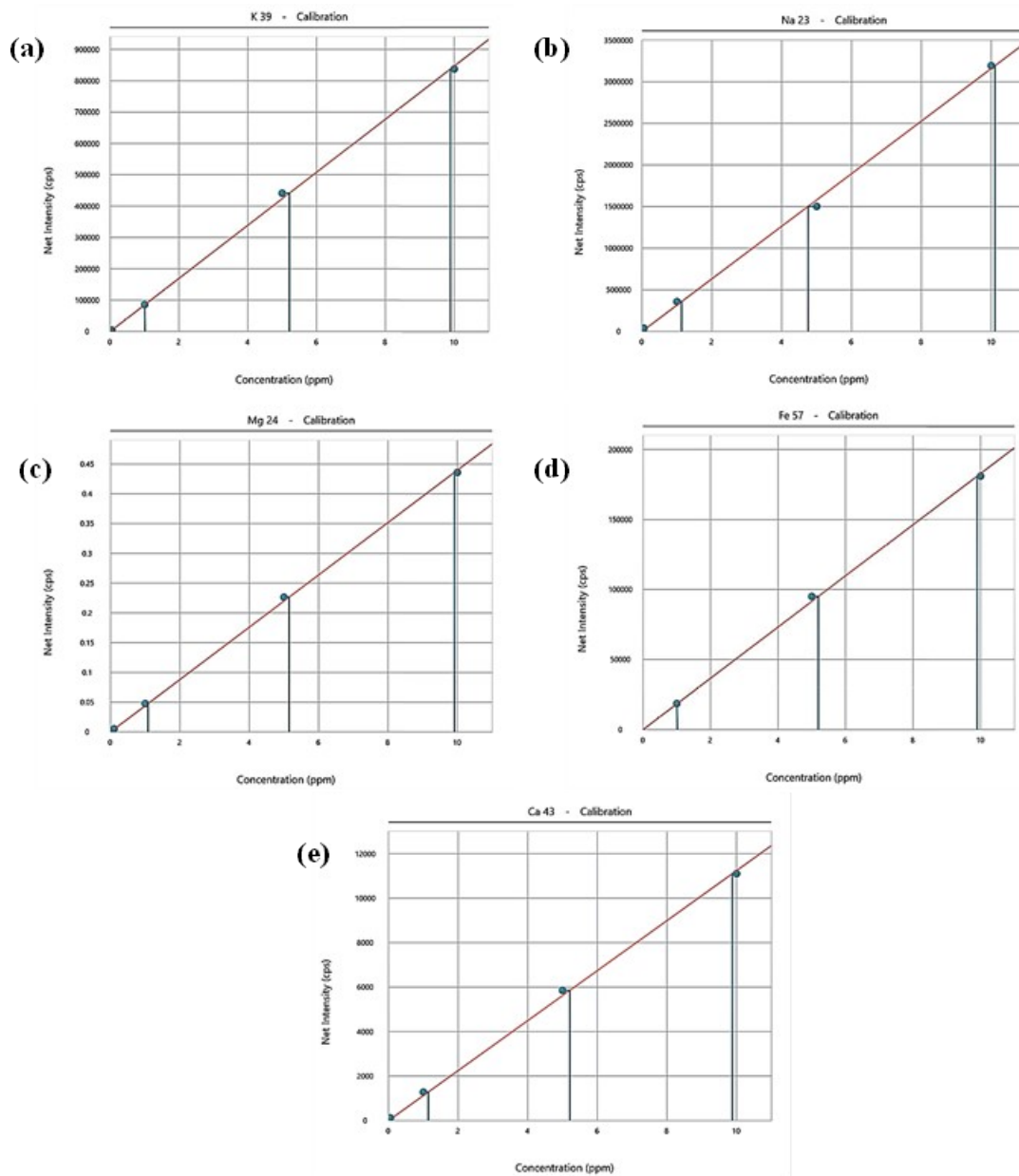


**Figure S6:** The elemental composition of the CT flower extract (a) Potassium; (b) Sodium; (c) Magnesium; (d) Iron; and (e) Calcium.

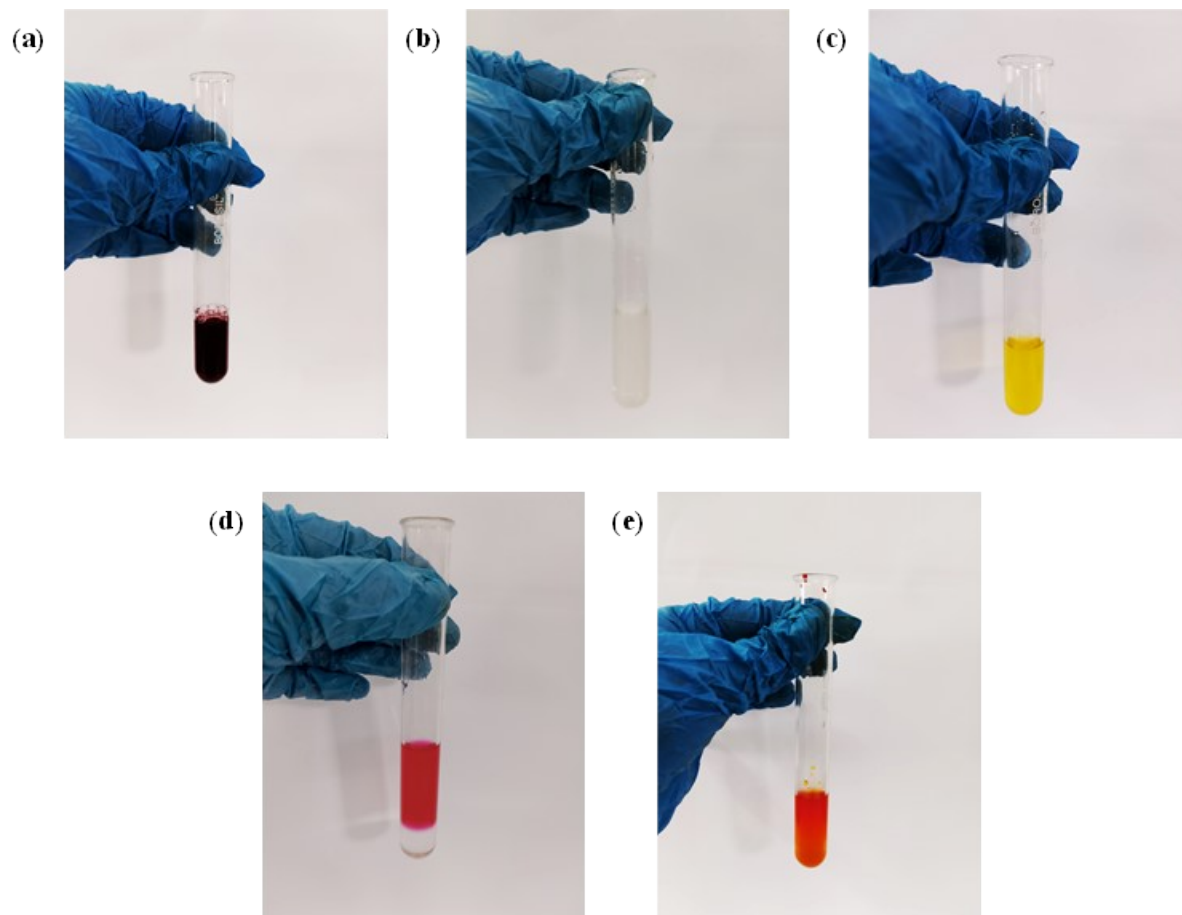


**Figure S7:** Tests to determine different bioactive compounds (a) phenolic compounds; (b) Alkaloids; (c) Flavonoids; (d) terpenoids and steroids; and (e) Cardiac glycosides.

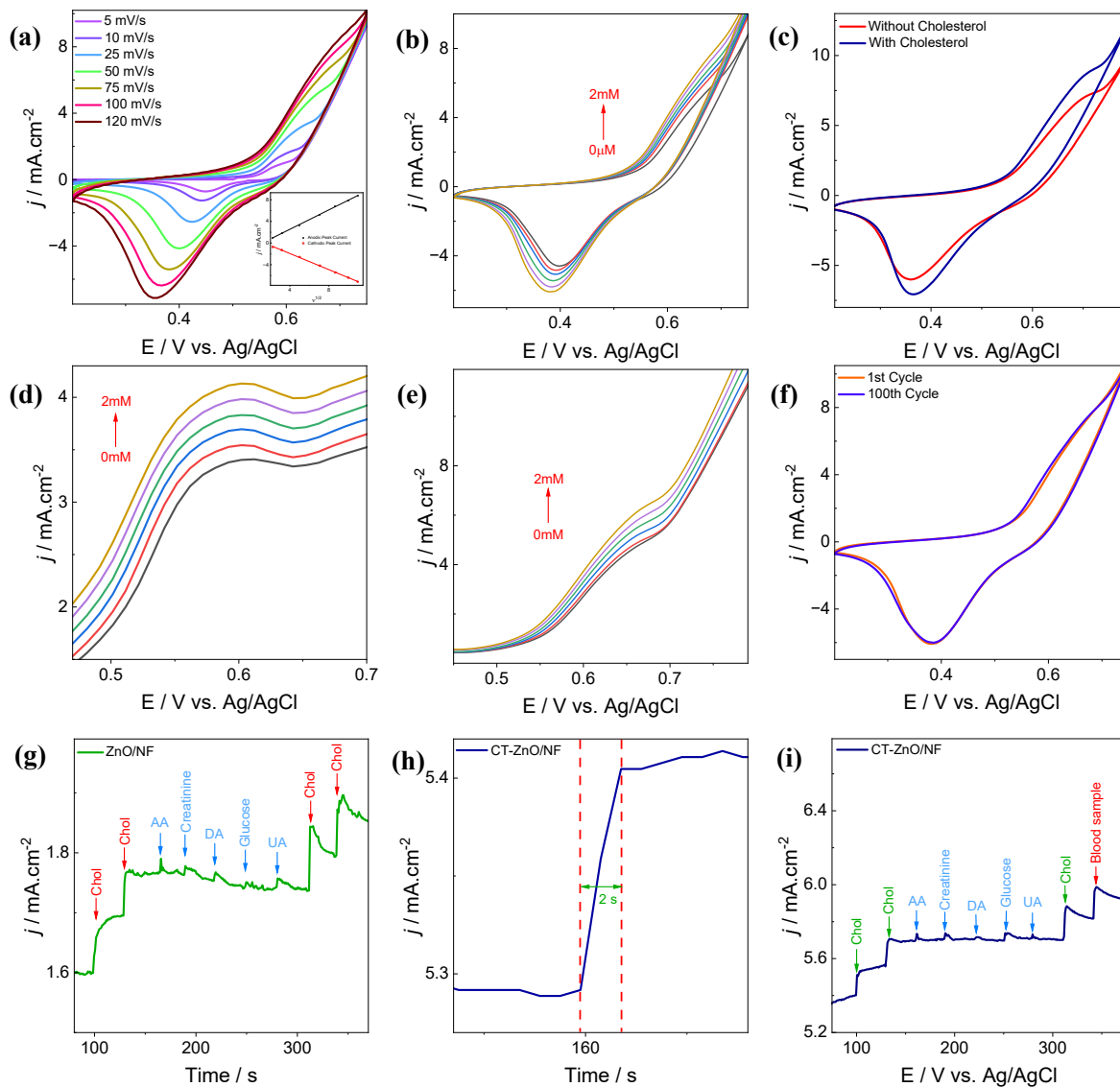


**Figure S8:** (a) Scan rate study of ZnO/NF in 0.1 M KOH from 5-120 mV/s. The anodic and cathodic peak currents are inserted as a function of the square root of the scan rate (inset); (b) The successive addition analysis for ZnO/NF at the scan rate of 50 mV/s; (c) CV of CT-ZnO/NF in the presence and absence of cholesterol at the scan rate of 50 mV/s; (d) DPV study of ZnO/NF to analyse the electrochemical response to successive cholesterol additions; (e) LSV study of ZnO/NF to analyse the electrochemical reaction to successive cholesterol additions. (f) CVs of ZnO/NF for 100 cycles in a 0.1 M KOH solution containing 2 mM cholesterol, with an applied potential scan rate of 50 mV/s; (g) An interference study of ZnO/NF under stirring conditions to assess its reaction to various interfering species at a potential of +0.64 V; (h) Response time plot of CT-ZnO/NF; (i) Interference study of CT-ZnO/NF with 1 mM concentration of different interfering species.

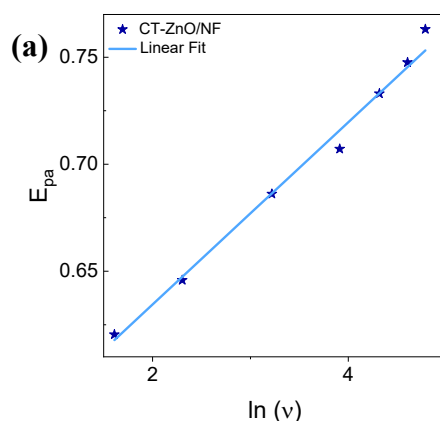


**Figure S9:** (a) Laviron Equation for CT-ZnO/NF.

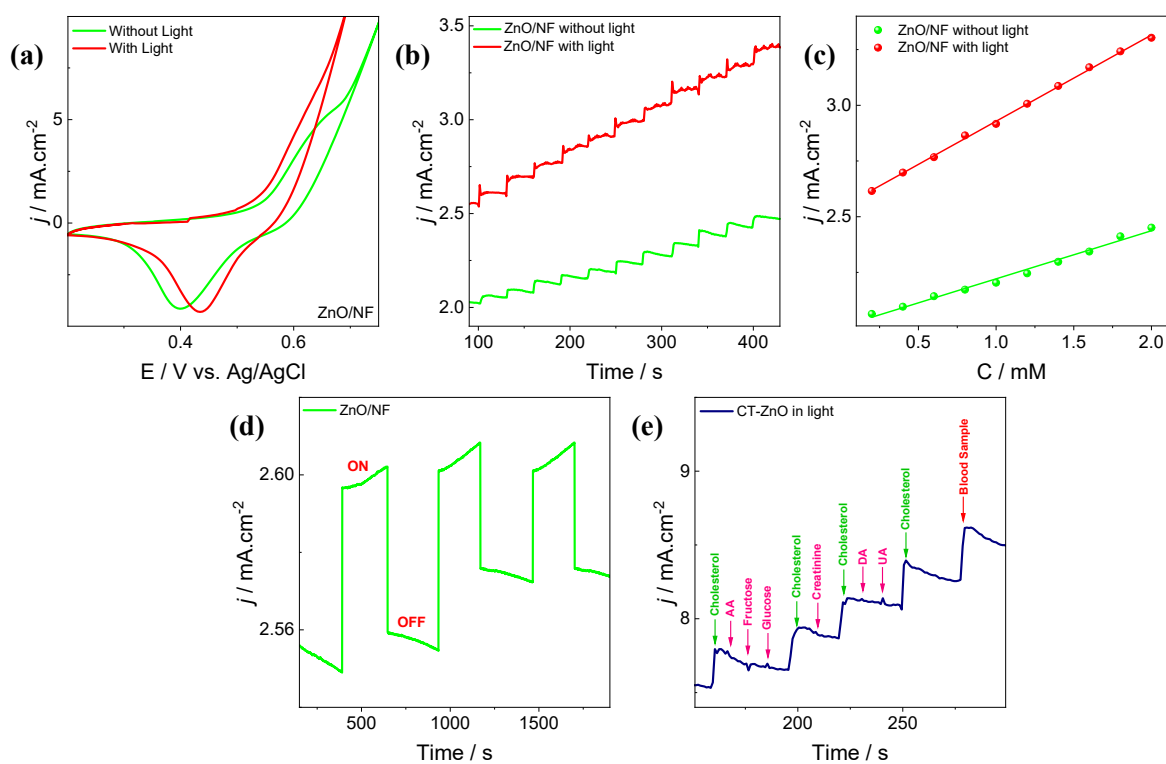


**Figure S10:** (a) CV analysis of ZnO/NF in with and without light, respectively, at the scan rate of 50 mV/s; (b) CA investigation of ZnO/NF was performed in a 0.1 M KOH solution, while stirring along with an applied potential of +0.69 V; (c) Calibration plot of ZnO/NF to estimate cholesterol; (d) Photocurrent analysis of ZnO/NF in dark and illuminated mode at +0.69 V of potential; (e) Interference analysis of CT-ZnO at +0.69 V under continuous stirring in the presence of light.

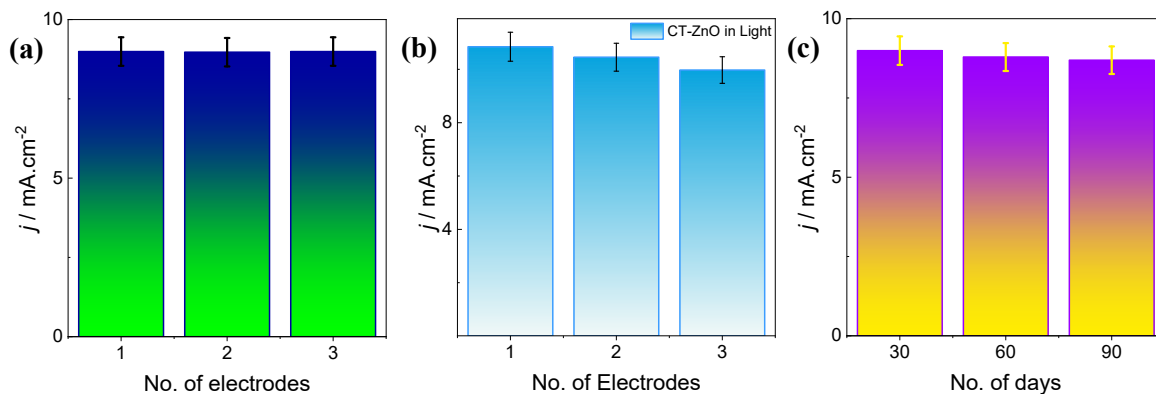


**Figure S11:** (a) Reproducibility was assessed using three different CT-ZnO/NF electrodes; (b) Reproducibility of CT-ZnO/NF utilizing 3 different electrodes in the presence of light; (c) The stability of the CT-ZnO/NF electrode was evaluated for 90 days.

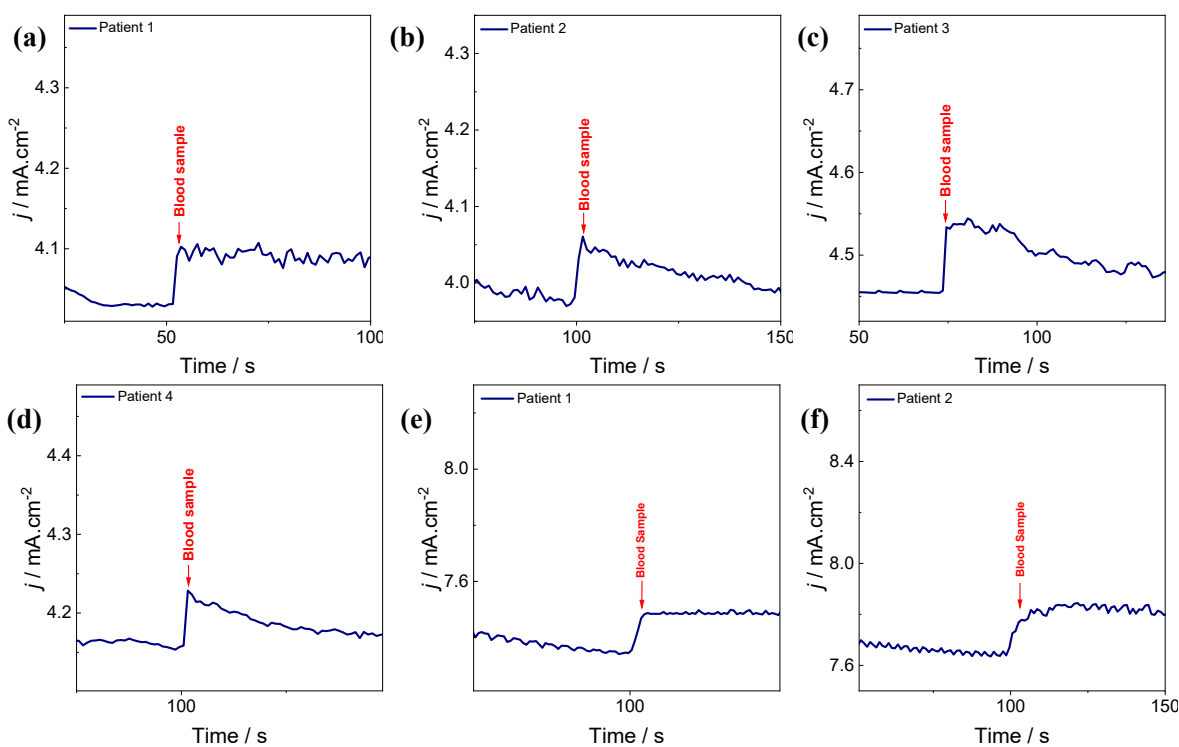


**Figure. S12:** (a-d) CA analysis of hydrolysed human blood serum in the absence of light; (e, f) CA analysis of hydrolysed human blood serum in the presence of light.

## References

- 1 H. Kim, Y. Lee, D. Song, Y. Kwon, E.-J. Kim and E. Cho, *Sustainable Energy Fuels*, 2020, **4**, 5247–5253.
- 2 J. Junita, D. Jayalakshmi and J. D. Rodney, *International Journal of Hydrogen Energy*, 2023, **48**, 14287–14298.
- 3 L. Rao, J. D. Rodney, S. S, F. J. Mascarenhas, M. P. Nayak, B. C. Kim and B. R. Bhat, *Microchemical Journal*, 2025, **212**, 113371.
- 4 M. Chelly, S. Chelly, R. Zribi, H. Bouaziz-Ketata, R. Gdoura, N. Lavanya, G. Veerapandi, C. Sekar and G. Neri, *Nanomaterials*, 2021, **11**, 739.
- 5 A. Padmapriya, P. Thiyagarajan, M. Devendiran, R. A. Kalaivani and A. M. Shanmugharaj, *Journal of Electroanalytical Chemistry*, 2023, **943**, 117609.
- 6 S. Kaveh, B. Norouzi, N. Nami and A. Mirabi, *J Mater Sci: Mater Electron*, 2021, **32**, 8932–8943.
- 7 V. Kumar, K. Singh, S. Panwar and S. K. Mehta, *Int Nano Lett*, 2017, **7**, 123–131.
- 8 M. S. Gijare, S. R. Chaudhari, S. Ekar, S. F. Shaikh, A. M. Al-Enizi, B. Pandit and A. D. Garje, *Journal of Photochemistry and Photobiology A: Chemistry*, 2024, **450**, 115434.
- 9 M. Chandrashekaraiyah, L. Ranganatha Venkataravanappa, S. T. Lakshmi Narayan Patel, P. C. Shivalingaiah, P. K. Ravi Shankar, N. Ganganagappa, N. P. H. Shivabasappa and S. B. Siddegowda, *Ionics*, 2026, **32**, 867–885.
- 10M. Zhang, Z. Qi, B. You, Y. Wang, Y. Wang and Z. Zhang, *Journal of Environmental Chemical Engineering*, 2025, **13**, 119565.